

Lithium and Aluminum Anthracenyldiimidatosulfates

Thomas Schulz and Dietmar Stalke

Institut für Anorganische Chemie, Georg-August Universität Göttingen, Tammannstraße 4,
37077 Göttingen, Germany

Reprint requests to Prof. Dr. D. Stalke. Fax: 0551/393459. E-mail: dstalke@chemie.uni-goettingen.de

Z. Naturforsch. **2010**, *65b*, 701–710; received February 9, 2010

9,10-Dibromo-anthracene was lithiated once or twice, and the products were reacted with different sulfur diimides. The reactions yielded [(THF)₂Li(N^tBu)₂SAnBr] (**1**), [(Et₂O)(LiBr)Li(N^tBu)₂-SAnBr]₂ (**2**), [Me₂Al(N^tBu)₂SAnBr] (**3**), [{(THF)₂Li(NR)₂S}]₂An] (**4**: R = ^tBu; **5**: R = SiMe₃) and [Me₂Al(NSiMe₃)₂S]₂An] (**6**). All products were fully characterized by X-ray structure analysis, elemental analysis, NMR and mass spectroscopy. From the solution NMR spectra it is evident that the rotation about the S–C bond is hindered even at r. t. leaving all protons of the anthracene framework non-equivalent.

Key words: Sulfur, Imide, Anthracene, Lithium, Aluminum

Introduction

It is known that heterobimetallic complexes might exhibit synergetic effects unreached by complexes with a single metal atom [1–7]. By the linkage of two coordination sites it is feasible to design ligands that are capable of coordinating two different metals. These bimetallic complexes can be useful for catalytic reactions [8–10] or as conjugated organometallic complexes or polymers [11, 12]. Because di- and triimidatosulfates are known to be able to coordinate a variety of different metals and are also subject to SET processes [13–15] it seemed advantageous to synthesize coupled diimidatosulfates since the products might form useful complexes for catalytic applications [16, 17] and/or new materials [18, 19]. Since we already synthesized some coupled di- and triimidatosulfates [20–22] it became evident that the main problem is not the synthetic access to the coupled imidatosulfates but the subsequent selective metal exchange. Unfortunately, classical transmetalation attempts with metal halides or metal amides that work with lithium organylimidatosulfates did not yield the expected products when applied to the coupled lithium imidatosulfates. Even if a reaction proceeds, not only one but both lithium atoms are exchanged leaving this route to heterobimetallic complexes closed [20]. To circumvent this problem the idea was to employ an organic spacer with two halogen atoms that can be selectively lithiated at one position first. After the lithiation the product

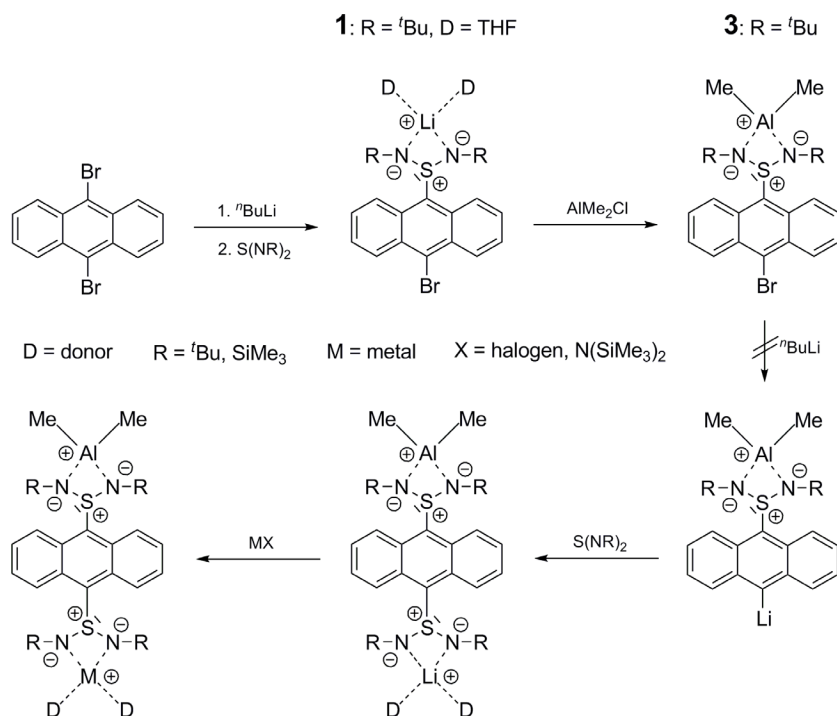
could be added to one equivalent of sulfurimide, and a metal exchange reaction (*e. g.* with Me₂AlCl) could be accomplished. After building up the first metal site a second lithiation and addition of a second sulfurimide should yield the desired heterobimetallic complex according to Scheme 1.

Earlier investigations have shown the selective lithiation of only one of the two bromine atoms in 9,10-dibromoanthracene to be feasible [23]. In addition, Schwab succeeded in substituting one bromine atom by a phosphanyl unit and could afterwards also lithiate the second bromine atom [24]. Therefore, 9,10-dibromoanthracene seemed to be an interesting spacer for the coupling of two imidatosulfate coordination sites. The results of our experiments with this organic spacer are presented here.

Results and Discussion

Synthesis of [(THF)₂Li(N^tBu)₂SAnBr] (1), [(Et₂O)(LiBr)Li(N^tBu)₂SAnBr]₂ (2) and [Me₂Al(N^tBu)₂SAnBr] (3) (An = anthracenyl, C₁₄H₈)

In a first series of experiments we lithiated 9,10-dibromoanthracene at one of the two positions with ⁿBuLi and reacted the product with di-*tert*-butylsulfur diimide (Scheme 1). The reactions proceeded smoothly and afforded [(THF)₂Li(N^tBu)₂SAnBr] (**1**) and [(Et₂O)(LiBr)Li(N^tBu)₂SAnBr]₂ (**2**) (An = anthracenyl, C₁₄H₈) depending on the elapsed reaction time and temperature. If the temperature had risen too



Scheme 1. Possible reaction pathway to coupled heterobimetallic diimidosulfates.

high (ca. 40 °C) during the lithiation or if the reaction time was too long, the lithiated anthracene reacted with the formed ⁿBuBr resulting in the formation of LiBr. In the following crystallization the lithium bromide was then incorporated in the solid-state structure of the formed anthracenyldiimidosulfate resulting in the formation of **2**. After the isolation of the anthracenyldiimidosulfates, **1** was transmetalated with one equivalent of Me₂AlCl. The reaction proceeded smoothly and yielded [Me₂Al(ⁿBu)₂SAnBr] (**3**).

Structural characterization of [(THF)₂Li(ⁿBu)₂SAnBr] (1), [(Et₂O)(LiBr)Li(ⁿBu)₂SAnBr]₂ (2) and [Me₂Al(ⁿBu)₂SAnBr] (3)

Table 1 contains selected bond lengths and angles for **1**, **2**, and **3**. Unexpectedly, [(THF)₂Li(ⁿBu)₂SAnBr] (**1**) crystallizes as a monomer with the lithium atom fourfold coordinated by the two nitrogen atoms of the diimidosulfate and two THF molecules (Fig. 1). Up to now diimidosulfates were known to give mostly dimeric structural motifs [25, 26] while monomeric structures were only formed in the presence of multidentate ligands like TMEDA, or by tripodal triimidosulfates [27, 28].

Since [(THF)₄Li₂{(NSiMe₃)₂S}₂biphenyl] also crystallizes as a monomer [20], it is anticipated that

Table 1. Selected bond lengths (Å) and angles (deg) for **1**, **2** and **3**.

| | 1 | 2 | 3 |
|-----------|----------|----------|----------|
| S–N1 | 1.602(4) | 1.641(3) | 1.643(2) |
| S–N2 | 1.603(4) | 1.613(3) | 1.641(2) |
| S–C | 1.860(5) | 1.832(3) | 1.815(3) |
| M1–N | 2.020(8) | 2.242(6) | 1.924(3) |
| | 2.009(8) | 1.977(6) | 1.920(2) |
| M2–N1 | | 1.971(6) | |
| Li–O/Al–C | 1.957(8) | 1.925(6) | 1.959(3) |
| | 1.947(8) | | 1.977(3) |
| Li1–Br | | 2.582(5) | |
| Li1a–Br | | 2.504(5) | |
| Li2–Br | | 2.496(6) | |
| N–S–N | 97.5(2) | 102.0(1) | 91.1(1) |
| N–M–N | 73.5(3) | 73.4(2) | 75.2(1) |
| C–S–N | 108.1(2) | 108.3(1) | 108.6(1) |
| | 107.5(2) | 103.5(1) | 110.3(1) |

one reason for this uncommon structural motif is the aryl group connected to the sulfur atom. The biphenyl and the anthracene substituent both can form C–H...π hydrogen bonds. A closer look at the packing diagram of both structures reveals intermolecular hydrogen bonds with a distance of about 3 Å between the hydrogen atoms of the THF molecules and the π systems of the next molecule, clearly in the region of weak hydrogen bonds [29]. [(THF)_{1.5}Li₂{(NSiMe₃)₂S}₂-biphenyl]_∞, the coordination polymer analog to

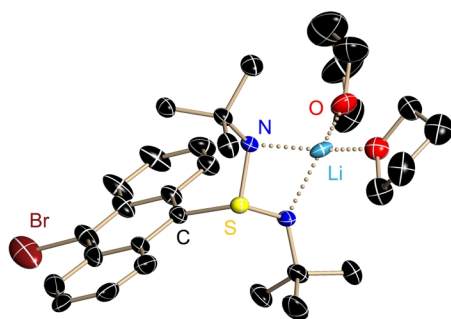


Fig. 1 (color online). Crystal structure of $[(\text{THF})_2\text{Li}(\text{N}^t\text{Bu})_2\text{SAnBr}]$ (**1**). Anisotropic displacement parameters are depicted at the 50% probability level, and all hydrogen atoms have been omitted for clarity.

monomeric $[(\text{THF})_4\text{Li}_2\{(\text{NSiMe}_3)_2\text{S}\}_2\text{biphenyl}]$, exhibits no intermolecular but similar intramolecular hydrogen bonds. Upon dimerization or polymerization the formation of weak intermolecular hydrogen bonds in the solid-state is not favored.

For **1** it seems advantageous to change the coordination mode of the lithium atoms to obtain a maximum of interactions between hydrogen atoms and the π system of the aryl groups because the formation of a potential aggregate would minimize the lattice energy contribution of the weak $\text{C}-\text{H}\cdots\pi$ hydrogen bonds.

In contrast to **1**, $[(\text{Et}_2\text{O})(\text{LiBr})\text{Li}(\text{N}^t\text{Bu})_2\text{SAnBr}]_2$ (**2**) crystallizes as a dimer with one equivalent of lithium bromide per molecule. Although a similar structure is known for the silver triimidosulfite [30], **2** is the first diimidosulfate crystallizing with incorporated lithium bromide. It forms a stair-shaped structure in the solid-state reminiscent of other structural motifs that are common for diimidosulfates [31–33]. Li1 and Li1a, the lithium atoms in the inner part of the stair, both exhibit a distorted tetrahedral coordination geom-

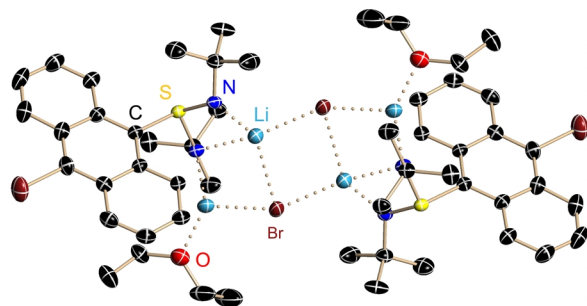


Fig. 2 (color online). Crystal structure of $[(\text{Et}_2\text{O})(\text{LiBr})\text{Li}(\text{N}^t\text{Bu})_2\text{SAnBr}]_2$ (**2**). Anisotropic displacement parameters are depicted at the 50% probability level, and all hydrogen atoms have been omitted for clarity.

etry like the lithium atoms in **1** while Li2 and Li2a are in an almost trigonal planar coordination (Fig. 2).

Table 1 shows that the lithium atoms in **1** are much more symmetrically coordinated than those in **2**. Since in known lithium diimidosulfates one nitrogen atom is always singly coordinated and the second doubly coordinated by lithium atoms, the coordination is normally very unsymmetrical which results in different S–N bond lengths. In **1** they are untypically similar and relatively short. Since both nitrogen atoms are only coordinated to one lithium atom there is enough electron density left to electrostatically reinforce the sulfur nitrogen bonds. The short S–N bond lengths result in an acute N–S–N angle since the sulfur lithium distances would otherwise be too short. The same holds true for **3** where the short Al–N bond lengths are responsible for the relatively sharp N–S–N angle of $75.15(8)^\circ$ (Fig. 3). So it is obvious that the structure of **1** is reminiscent of that of other monomeric imidosulfates or $[(\text{tmeda})\text{Li}(\text{N}^t\text{Bu})_2\text{S}(\text{SC}_8\text{H}_5)]$ [29] rather than of dimeric lithium diimidosulfates.

On the other hand, **2** is very similar to known lithium diimidosulfates with nearly all bond lengths and angles of about the values known from the literature. As expected all bond lengths to Li2 are shorter than the comparable ones to Li1 since Li2 exhibits only three donors. One of the C–S–N bond angles is very acute compared to the other C–S–N angles in Table 1. This is probably due to the position of the second lithium atom forcing the diimido ligand to bend to this side of the anthracene substituent.

As pointed out earlier, **3** exhibits the same structural motif as **1** (Figs. 1 and 3). Only the S–N and the N–M bond lengths differ slightly because of the metal exchange from lithium to aluminum. The aluminum atom

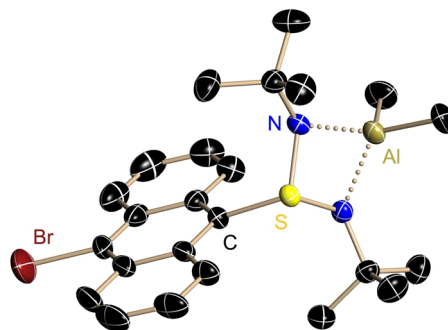
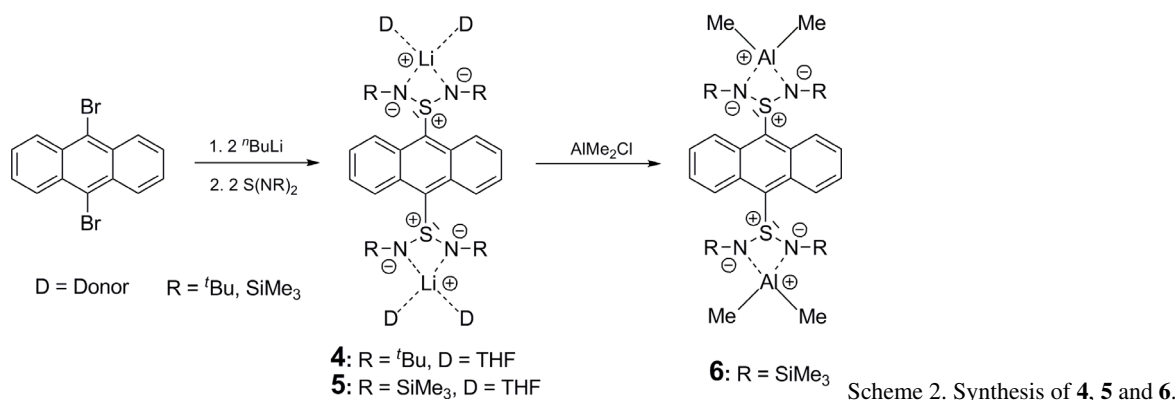


Fig. 3 (color online). Crystal structure of $[\text{Me}_2\text{Al}(\text{N}^t\text{Bu})_2\text{SAnBr}]$ (**3**). Anisotropic displacement parameters are depicted at the 50% probability level, and all hydrogen atoms have been omitted for clarity.



is more strongly coordinated by the nitrogen atoms resulting in a shorter N–M and a longer S–N distance.

Synthesis of $[(\text{THF})_2\text{Li}(\text{NR})_2\text{S}]_2\text{An}$ (**4**: R = ^tBu; **5**: R = SiMe₃) and $[\text{Me}_2\text{Al}(\text{NSiMe}_3)_2\text{S}]_2\text{An}$ (**6**)

Subsequent to the synthesis of **1–3** we tried to replace the remaining bromine atom in all three compounds by a lithium atom in a Gilman reaction. **1–3** were reacted with classical lithium organics (ⁿBuLi, MeLi and ^tBuLi) in various solvents at different temperatures. Unfortunately, all the reactions did not yield the expected products, but only unidentifiable mixtures which were impossible to work up. A few side-products were isolated, unfortunately not providing any insight into the general course of the reaction. It seems that by the addition of the first electron-withdrawing sulfurdiiimide the electron density in the anthracenyl framework is reduced thus far that a second lithiation is not favored.

For that reason we abandoned the idea of a sequential lithiation and metalated both bromine positions in a single step. Afterwards 9,10-dilithiumanthracene was reacted with two differently substituted sulfurdiiimides (Scheme 2) resulting in the formation of **4** and **5**.

After isolation and purification, **4** and **5** were reacted with one equivalent of Me₂AlCl. With **4** the aluminum complex could not be obtained, but the reaction of **5** with Me₂AlCl afforded **6**. The NMR spectrum of the reaction mixture suggested a successful metal exchange, but the lack of crystals and the sensitivity of the product made an unequivocal characterization of the product impossible. In the reaction with Me₂AlCl both lithium atoms are exchanged by aluminum resulting in a bimetallic symmetrical complex rather than in a heterobimetallic species. This phenomenon was

already observed when benzene and biphenyl spacers were employed [20]. It seems that Me₂AlCl is too reactive and not selective enough to exchange just one lithium atom by salt elimination.

Structural characterization of $[(\text{THF})_2\text{Li}(\text{NR})_2\text{S}]_2\text{An}$ (**4**: R = ^tBu; **5**: R = SiMe₃) and $[\text{Me}_2\text{Al}(\text{NSiMe}_3)_2\text{S}]_2\text{An}$ (**6**)

4, **5**, and **6** crystallize as monomers with half of the molecule in the asymmetric unit (Figs. 4–6). They all exhibit the same structural motif. Table 2 contains selected bond lengths and angles for **4**, **5**, and **6**.

As described earlier in this paper, the diimidosulfates normally tend to dimerize in favor of the four-fold coordination at the lithium atom. Compound **1** breaks with this rule of thumb and so do **4** and **5**. The coordination of the metal atoms is analogous to the coordination in **1**. As expected, the coupled diimidosulfate groups are arranged *trans* to each other.

The main geometrical features of **1**, **4** and **5** show no distinct differences. **1** and **4** exhibit nearly the same bond lengths and angles, while **5** displays only

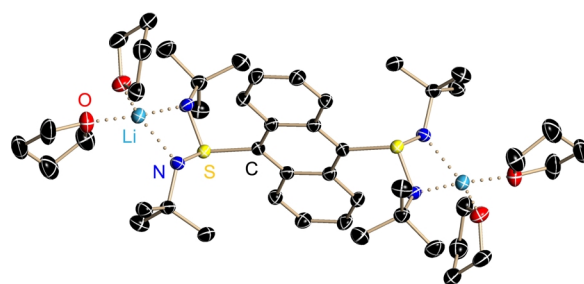
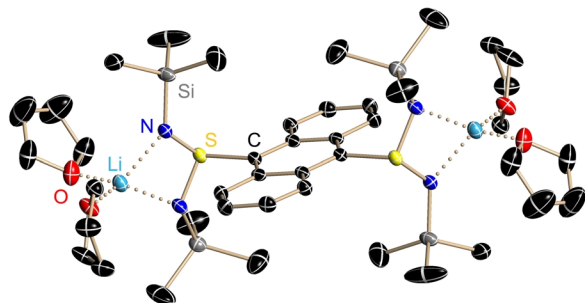
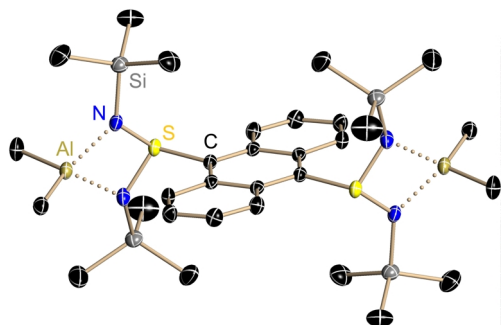


Fig. 4 (color online). Crystal structure of $[(\text{THF})_2\text{Li}(\text{N}^t\text{Bu})_2\text{S}]_2\text{An}$ (**4**). Anisotropic displacement parameters are depicted at the 50% probability level, and all hydrogen atoms have been omitted for clarity.

Table 2. Selected bond lengths (Å) and angles (deg) for **4**, **5** and **6**.

| | 4 | 5 | 6 |
|-----------|----------|----------|----------|
| S–N1 | 1.616(2) | 1.600(2) | 1.631(2) |
| S–N2 | 1.618(2) | 1.603(2) | 1.625(2) |
| S–C | 1.852(2) | 1.843(2) | 1.827(2) |
| M1–N | 2.022(4) | 2.038(4) | 1.944(2) |
| Li–O/Al–C | 1.996(4) | 2.043(4) | 1.944(2) |
| | 1.950(4) | 1.957(4) | 1.964(2) |
| | 1.953(5) | 1.936(4) | 1.964(2) |
| N–S–N | 98.1(1) | 101.9(1) | 94.8(1) |
| N–M–N | 74.9(2) | 75.1(1) | 76.1(1) |
| C–S–N | 106.0(1) | 106.3(1) | 109.4(1) |
| | 108.6(1) | 107.0(1) | 108.8(1) |

Fig. 5 (color online). Crystal structure of $[(\text{THF})_2\text{Li}(\text{NSiMe}_3)_2\text{S}]_2\text{An}$ (**5**). Anisotropic displacement parameters are depicted at the 50% probability level, and all hydrogen atoms have been omitted for clarity.Fig. 6 (color online). Crystal structure of $[\text{Me}_2\text{Al}(\text{NSiMe}_3)_2\text{S}]_2\text{An}$ (**6**). Anisotropic displacement parameters are depicted at the 50% probability level, and all hydrogen atoms have been omitted for clarity.

marginal deviations. Only the Li–N distances are slightly longer in **5** resulting also in a somewhat more acute N–S–N angle. These small differences probably arise from the change from the *tert*-butyl to the trimethylsilyl substituents on the nitrogen atoms.

The diimidosulfate substituents in the 9 and 10 position at the anthracenyl backbone do not bias the C_{14}H_8 moiety or influence each other.

Apparently the switch from the *tert*-butyl to the trimethylsilyl groups at the nitrogen atoms leads to a small elongation of the M–N bonds and a small contraction of the S–N distances. This might be an indication that more of the negative charge at the nitrogen atom is employed to strengthen the S–N bond because the positive charge at the metal is additionally stabilized by the β -effect of the silicon atom of the trimethylsilyl groups [34, 35].

NMR studies of the anthracenyldiimidosulfates

The NMR spectra of all compounds reveal an unexpected number of signals. For **1–3** four signals are expected with a 2:2:2:2 ratio for the protons at the anthracenyl framework, but integration shows that all eight protons are inequivalent for **1–3** (Fig. 7). For **4–6** the expected distribution of 4:4 is transformed into 2:2:2:2. This leads to the assumption that the rotation about the S–C bond is hindered even at r. t. A similar phenomenon was observed for isopropylphosphanyl-anthracenes [36]. Schwab *et al.* found that the rotation about the P–C bond is slow enough at low temperature to leave all protons magnetically and chemically different. In addition, one of the protons in close proximity to the phosphorus atom is fixed between the isopropyl groups while the proton on the other side can interact with its lone pair. The same situation seems to arise for the diimidosulfates with one proton being clamped by two nitrogen atoms. A NOESY experiment shows that the hydrogen atom pinched between both nitrogen atoms is the one with the highest chemical shift (H_5 : 10.15 ppm). Although the protons of the *t*Bu groups yield cross-peaks with H_5 and H_4 , only one cross-peak between H_5 and one of the methyl groups attached to the aluminum atom can be seen. This strongly indicates that **3** exhibits the same conformation (Fig. 7) in solution as in the solid-state.

For the bis(diimidosulfates) with the *tert*-butyl substituent at the nitrogen atoms the protons resonate differently even at r. t. while the bis(diimidosulfates) with the trimethylsilyl groups exhibit only very broad signals at 25 °C. By cooling **5** to –60 °C the broad signals can be resolved and show the anticipated pattern with the 2:2:2:2 ratio. This fact can be explained by the longer N–Si bonds (1.87 Å compared to 1.47 Å for N–C) facilitating a rotation about the S–C bonds. Unfortunately the 4J and the 5J coupling can still not be resolved. Furthermore the differences in the chemical shifts of the protons are bigger for the lithium

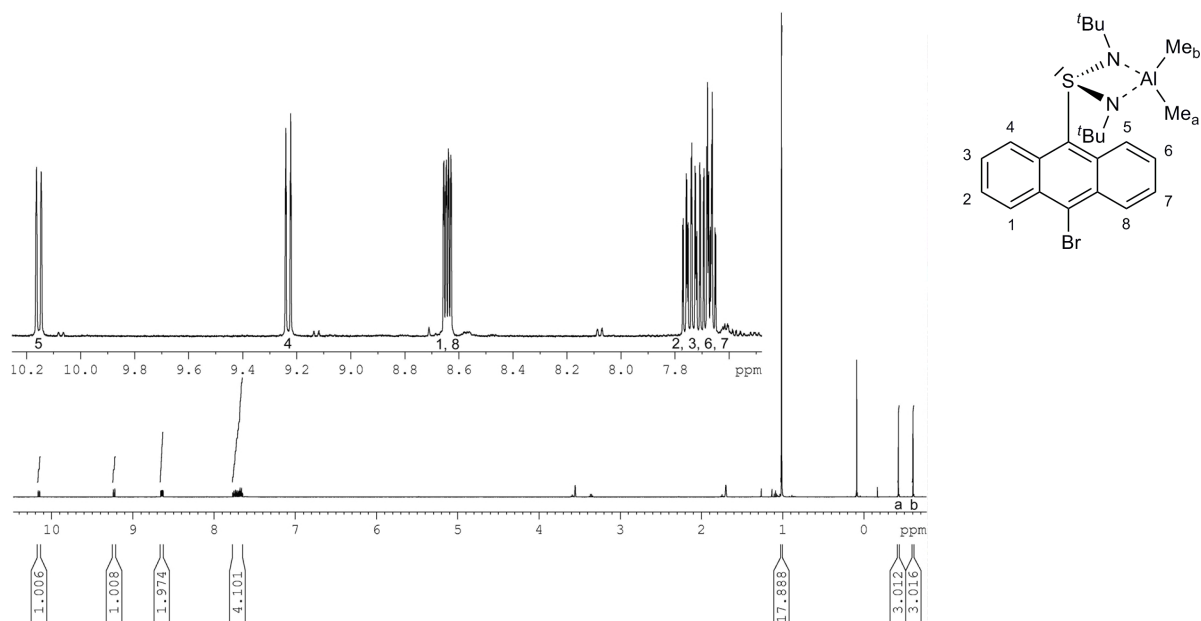


Fig. 7. ^1H NMR spectrum (left) and probable conformation in solution (right) of **3**.

than for the aluminum complexes. The reason for this is probably the higher steric demand of the THF-coordinated lithium cation compared to the AlMe_2 cation. A NOESY spectrum of **4** was recorded because this experiment enabled to determine the conformation of **3** in solution. Since the signals in the ^1H NMR spectrum of **4** at r. t. were still too broad the NOESY was recorded at -70°C . To our surprise it showed the singlet for the protons of the $t\text{Bu}$ groups to split up in four different signals as two pairs with the same integral intensity. Two different signals would count for the *transoid* or *cisoid* conformers each [36] which are then split again. The four $t\text{Bu}$ groups at both conformers become inequivalent at low temperatures to give rise to two signals. This is due to the fact that the sulfur lone pairs avoid to be arranged ideally in the anthracene plane. This causes the displacement of the NSN bisection out of the anthracene plane and the two groups to be magnetically inequivalent. This is further substantiated by the signals of the aromatic core. At low temperature the distribution of the integrated signals changes from originally 2:2:2:2 to 1:1:2:2. As expected the NOESY spectrum shows cross peaks between the signals for H_2 , H_3 , H_6 and H_7 and all other signals but no cross peaks between the other four aromatic hydrogen atoms. Unfortunately, there is no cross peak between the aromatic signals and the peaks for the $t\text{Bu}$ groups

making an assignment of the conformation in solution impossible.

Conclusion

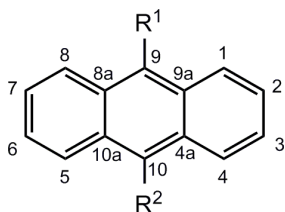
The experiments described in this paper show that 9,10-dibromoanthracene is a suitable candidate for the linkage of two sulfur diimide moieties. The resulting lithium bis(diimidosulfates) are obtained in good yields and easily undergo metal exchange reactions with Me_2AlCl . Unfortunately, the metal exchange with this very reactive organometallic reagent is not selective enough to serve as a starting material for heterobimetallic complexes. Further experiments with a variety of other metal halides and metal amides are necessary. In addition we found that 9,10-dibromoanthracene can be selectively lithiated at only one position and reacts cleanly with sulfur diimides to give a lithium diimidosulfate. The subsequent metal exchange reaction can be accomplished, but the stepwise synthesis of the heterobimetallic complex could not be realized. After one position of the anthracenyl framework is substituted, the second lithiation is hampered through the electron withdrawing effect of the first diimidosulfate. Therefore another spacer between the sulfur diimides has to be employed, or a different approach for the metal exchange must be found.

One option would be the hydrolysis of **4** or **5** with subsequent deprotonation with different metal amides or metal hydrides. This already proved to be a smooth way of synthesizing diimidatesulfate metal complexes. The anthracenyldiimidatesulfates show interesting features in the NMR spectra. The rotation about the S–C bond is hindered because of the bulky substituents at the nitrogen atoms.

Experimental Section

All experiments were carried out either in an atmosphere of purified, dry nitrogen or argon by using modified Schlenk techniques, or in an argon drybox. The glassware was dried for several hours at 120 °C, assembled hot and allowed to cool to r. t. while the vacuum was maintained. The solvents were freshly distilled from potassium prior to use and degassed. The reactants were commercially available or synthesized according to published procedures: S(*N*^tBu)₂ [37] and S(NSiMe₃)₂ [38].

All NMR spectra were recorded on a Bruker Avance 500 spectrometer. The chemical shifts δ are given in ppm with positive values for low-field shifts relative to tetramethylsilane as external standard. The numbering for the anthracene framework is shown below.



Elemental analyses were performed by the Mikroanalytisches Labor des Instituts für Anorganische Chemie der Universität Göttingen with an Elementar Vario EL3 apparatus. The determined values deviate more than usual from the calculated numbers as the substances are highly sensitive to oxygen and moisture and tend to lose coordinated THF.

Mass spectra were recorded with the electron ionization method (EI-MS: 70 eV) on a Finnigan MAT 95 spectrometer. The mass-to-charge ratios (*m/z*) of the fragment ions are based on the molecular mass of the isotopes with the highest natural abundance. The molecular ion peak *M* is defined as the compound without coordinated solvent, and in the case of lithium complexes also without the lithium atom. Some spectra were unspecific as the ionic character and the lability of the synthesized compounds made the measurements difficult. Due to the reactivity and solubility of the compounds no electron spray ionization (ESI-MS) or fast atom bombardment (FAB-MS) mass spectra could be recorded.

Synthesis of [(THF)₂Li(*N*^tBu)₂SA*n*Br] (**1**)

ⁿBuLi (1.37 mL, 2.22 M, 3.04 mmol) is added dropwise to a suspension of 9,10-dibromoanthracene (1.00 g, 2.98 mmol) in 25 mL of diethyl ether at –15 °C. The reaction mixture is stirred for 30 min before addition of *N,N'*-di-*tert*-butylsulfurdiimide (1.04 g, 2.98 mmol). The suspension is stirred for 30 min, and insoluble products are removed by filtration. After removal of the solvent, the product is obtained as a red powder. Crystals are obtained from a saturated solution in THF upon a few days storage at 4 °C. Yield (%): 1.33 g, 2.28 mmol, 76 %. – Elemental analysis in % found (calcd.): C 61.90 (61.96), H 7.21 (7.28), N 5.05 (4.82), S 5.71 (5.51). – ¹H NMR (500 MHz, [D₈]THF): δ = 10.59 (ddd, ³*J*_{HH} = 8.98 Hz, ⁴*J*_{HH} = 1.19 Hz, ⁵*J*_{HH} = 0.73 Hz, 1 H, H₅), 9.44 (ddd, ³*J*_{HH} = 8.68 Hz, ⁴*J*_{HH} = 1.44 Hz, ⁵*J*_{HH} = 0.70 Hz, 1 H, H₄), 8.44 (ddd, ³*J*_{HH} = 8.66 Hz, ⁴*J*_{HH} = 1.60 Hz, ⁵*J*_{HH} = 0.73 Hz, 1 H, H₈), 8.42 (ddd, ³*J*_{HH} = 9.21 Hz, ⁴*J*_{HH} = 1.42 Hz, ⁵*J*_{HH} = 0.77 Hz, 1 H, H₁), 7.52–7.44 (m, 3 H, H₇, H₃, H₂), 7.26 (ddd, ³*J*_{HH} = 8.96 Hz, ³*J*_{HH} = 6.44 Hz, ⁴*J*_{HH} = 1.26 Hz, 1 H, H₆), 3.62 ppm (m, 8 H, OCH₂CH₂), 1.77 (m, 8 H, OCH₂CH₂), 0.95 (s, 18 H, C(CH₃)₃). – ¹³C{¹H} NMR (125 MHz, [D₈]THF): δ = 155.9 (s, C₁₀), 132.0–130.7 (s, C_{10a}, C_{4a}, C_{9a}, C_{8a}), 128.8 (s, C₈), 128.2 (s, C₅), 128.1 (s, C₄), 127.6–125.6 (s, C₇, C₃, C₂), 125.2 (s, C₁), 123.5 (s, C₉), 123.3 (s, C₆), 67.4 (OCH₂CH₂), 52.9 (s, C(CH₃)₃), 33.8 (s, C(CH₃)₃), 25.3 (OCH₂CH₂). – EI-MS: *m/z* (% = 303 (32) [M–*N*^tBu–^tBu+H]⁺, 288 (20) [M–2 *N*^tBu]⁺, 256 (100) [M–S(*N*^tBu)₂]⁺, 178 (58) [anthracene]⁺, 118 (35) [M–anthracene–Br–^tBu+2 H]⁺, 103 (32) [M–anthracene–Br–*N*^tBu+H]⁺, 57 (100) [^tBu]⁺.

Synthesis of [(Et₂O)(LiBr)Li(*N*^tBu)₂SA*n*Br]₂ (**2**)

ⁿBuLi (1.37 mL, 2.22 M, 3.04 mmol) is added dropwise to a suspension of 9,10-dibromoanthracene (1.00 g, 2.98 mmol) in 25 mL of diethyl ether at –15 °C. The reaction mixture is allowed to warm to r. t. and stirred for 4 h before addition of *N,N'*-di-*tert*-butylsulfurdiimide (1.04 g, 2.98 mmol). The suspension is stirred for 30 min, and insoluble products are removed by filtration. From this solution crystals are obtained after a few days storage at 4 °C. For **2** the highest peaks in the mass spectrum and the peaks shown in the NMR spectrum were the same as for **1**. The elemental analysis for **2** gave poor results. Yield (%): 0.99 g, 1.65 mmol, 55 %.

Synthesis of [Me₂Al(*N*^tBu)₂SA*n*Br] (**3**)

AlMe₂Cl (0.3 mL, 3 mmol) is added dropwise to a solution of **1** (2.27 g, 3 mmol) in 10 mL THF at –78 °C. The reaction mixture is allowed to warm to r. t. and stirred for 4 h. Insoluble products are removed by filtration, and the solution is stored at 4 °C. Orange crystals suitable for X-ray diffraction experiments are obtained after a few days

of storage. Yield (%): 1.07 g, 2.2 mmol, 73 %. – Elemental analysis in % found (calcd.): C 58.67 (59.14), H 6.57 (6.57), N 5.93 (5.75), S 6.60 (6.57). – ^1H NMR (500 MHz, $[\text{D}_8]\text{THF}$): δ = 10.15 (ddd, $^3J_{\text{HH}}$ = 8.92 Hz, $^4J_{\text{HH}}$ = 1.21 Hz, $^5J_{\text{HH}}$ = 0.80 Hz, 1 H, H₅), 9.23 (ddd, $^3J_{\text{HH}}$ = 9.03 Hz, $^4J_{\text{HH}}$ = 1.10 Hz, $^5J_{\text{HH}}$ = 0.73 Hz, 1 H, H₄), 8.65 (ddd, $^3J_{\text{HH}}$ = 8.89 Hz, $^4J_{\text{HH}}$ = 1.33 Hz, $^5J_{\text{HH}}$ = 0.69 Hz, 1 H, H₈), 8.64 (ddd, $^3J_{\text{HH}}$ = 8.83 Hz, $^4J_{\text{HH}}$ = 1.34 Hz, $^5J_{\text{HH}}$ = 0.71 Hz, 1 H, H₁), 7.77–7.65 (m, 4 H, H₇, H₆, H₃, H₂), 1.01 (s, 18 H, C(CH₃)₃), –0.42 (s, 3 H, Al(CH₃)₂), –0.60 (s, 3 H, Al(CH₃)₂). – $^{13}\text{C}\{^1\text{H}\}$ NMR (125 MHz, $[\text{D}_8]\text{THF}$): δ = 136.1 (s, C₁₀), 134.0 (s, C₉), 131.7–130.9 (s, C_{10a}, C_{4a}, C_{9a}, C_{8a}), 129.9 (s, C₈), 129.3 (s, C₁), 129.5–127.7 (s, C₇, C₆, C₃, C₂), 125.6 (s, C₅), 122.7 (s, C₄), 53.8 (s, C(CH₃)₃), 31.7 (s, C(CH₃)₃), –4.6 (s, Al(CH₃)₂), –5.2 (s, Al(CH₃)₂). – EI-MS: m/z (%) = 473 (100) $[\text{M}-\text{Me}]^+$, 402 (42) $[\text{M}-\text{N}^t\text{Bu}-\text{Me}+\text{H}]^+$, 359 (32) $[\text{M}-\text{N}^t\text{Bu}-\text{AlMe}_2]^+$, 345 (31) $[\text{M}-\text{N}^t\text{Bu}-\text{Me}-^t\text{Bu}+\text{H}]^+$, 330 (29) $[\text{M}-2\text{N}^t\text{Bu}-\text{Me}]^+$, 250 (27) $[\text{M}-\text{N}^t\text{Bu}-\text{Me}-^t\text{Bu}-\text{Br}+\text{H}]^+$.

Synthesis of $[(\text{THF})_2\text{Li}(\text{NR})_2\text{S}]_2\text{An}$ (4: R = ^tBu ; 5: R = SiMe_3)

$^n\text{BuLi}$ (2.74 mL, 2.22 M, 6.08 mmol) is added dropwise to a suspension of 9,10-dibromoanthracene (1.00 g, 2.98 mmol) in 25 mL of diethyl ether at -15°C . The reaction mixture is stirred for 30 min, and the dilithiated anthracene is isolated by filtration. Yield: 0.78 g, 2.3 mmol, 77 %. N,N' -bis-*tert*-butyl-sulfurdiimide (0.80 g, 4.6 mmol) (**4**) or N,N' -bis-trimethylsilyl-sulfurdiimide (0.86 g, 4.6 mmol) (**5**) is added drop wise to a solution of the dilithiated anthracene (0.78 g, 2.3 mmol) in 10 mL THF at -78°C . The reaction mixture is allowed to warm to r. t. and stirred for 4 h. Insoluble products are removed by filtration. Crystals are obtained from the saturated solution upon a few days storage at 4°C .

4: Yield (%): 1.65 g, 1.7 mmol, 74 %. Elemental analysis in % found (calcd.): C 65.82 (66.78), H 8.88 (9.42), N 7.86 (6.23), S 9.13 (7.13). – ^1H NMR (500 MHz, $[\text{D}_8]\text{THF}$): δ = 10.24 (br, 2 H, H₁, H₅), 8.91 (br, 2 H, H₈, H₄), 7.61 (br, 4 H, H₆, H₂, H₃, H₇), 3.62 ppm (m, 16 H, OCH₂CH₂), 1.77 (m, 16 H, OCH₂CH₂), 1.29 (s, 18 H, C(CH₃)₃), 1.14 (s, 18 H, C(CH₃)₃). – $^{13}\text{C}\{^1\text{H}\}$ NMR (125 MHz, $[\text{D}_8]\text{THF}$): δ = 142.6 (s, C₁₀, C₉), 129.1 (br, C₁, C₅), 128.7–128.2 (m, C_{10a}, C_{4a}, C_{9a}, C_{8a}), 127.7–126.4 (m, C₆, C₂, C₃, C₇), 124.7 (s, C₄, C₈), 67.4 (OCH₂CH₂), 56.7 (s, C(CH₃)₃), 54.5 (s, C(CH₃)₃), 33.6 (s, C(CH₃)₃), 31.0 (s, C(CH₃)₃), 25.3 (OCH₂CH₂). – EI-MS: m/z (%) = 312 (22) $[\text{M}-3\text{N}^t\text{Bu}+\text{H}]^+$, 256 (28) $[\text{M}-3\text{N}^t\text{Bu}-^t\text{Bu}+2\text{H}]^+$, 118 (25) $[\text{SN}^t\text{BuNH}]^+$, 103 (28) $[\text{SN}^t\text{Bu}]^+$, 57 (100) $[\text{N}^t\text{Bu}]^+$, 41 (44) $[\text{CH}_2\text{CCH}_3]^+$.

5: Yield (%): 1.47 g, 1.65 mmol, 72 %. – Elemental analysis in % found (calcd.): C 56.36 (56.59), H 9.10 (8.59), N 6.35 (6.29), S 7.44 (7.19). – ^1H NMR (500 MHz, $[\text{D}_8]\text{THF}$): δ = 10.29 (d, $^3J_{\text{HH}}$ = 8.00 Hz, 2 H, H₁, H₅),

9.29 (d, $^3J_{\text{HH}}$ = 9.40 Hz, 2 H, H₈, H₄), 7.44–7.28 (m, 2 H, H₆, H₂), 7.29–7.23 (m, 2 H, H₃, H₇), 3.62 ppm (m, 16 H, OCH₂CH₂), 1.77 (m, 16 H, OCH₂CH₂), –0.40 (s, 36 H, Si(CH₃)₃). – $^{13}\text{C}\{^1\text{H}\}$ NMR (125 MHz, $[\text{D}_8]\text{THF}$): δ = 151.4 (s, C₁₀, C₉), 130.9–129.4 (m, C_{10a}, C_{4a}, C_{9a}, C_{8a}), 127.1 (s, C₁, C₅), 125.2 (s, C₆, C₂), 124.2 (s, C₄, C₈), 123.2 (s, C₃, C₇), 67.4 (OCH₂CH₂), 25.3 (OCH₂CH₂), 2.5 (s, Si(CH₃)₃). – EI-MS: m/z (%) = 264 (64) $[\text{M}-4\text{Me}]^+$, 191 (100) $[\text{M}-\text{S}(\text{NSiMe}_3)_2]^+$, 207 (20) $[\text{S}(\text{NSiMe}_3)_2+\text{H}]^+$, 178 (24) $[\text{anthracene}]^+$, 73 (65) $[\text{SiMe}_3]^+$.

Synthesis of $[\text{Me}_2\text{Al}(\text{NSiMe}_3)_2\text{S}]_2\text{An}$ (6)

AlMe_2Cl (0.3 mL, 3 mmol) is added dropwise to a solution of **5** (2.67 g, 3 mmol) in 10 mL THF at -78°C . The reaction mixture is allowed to warm to r. t. and stirred for 4 h. Insoluble products are removed by filtration, and the solution is stored at 4°C . Crystals suitable for X-ray diffraction experiments are obtained after a few days of storage. Yield (%): 0.84 g, 1.2 mmol, 40 %. Elemental analysis in % found (calcd.): C 49.82 (51.24), H 7.92 (8.03), N 7.73 (7.97), S 8.73 (9.12). – ^1H NMR (500 MHz, $[\text{D}_8]\text{THF}$): δ = 10.21 (br, 2 H, H₁, H₅), 9.29 (br, 2 H, H₈, H₄), 7.85–7.72 (m, 4 H, H₆, H₂, H₃, H₇), –0.20 (s, 36 H, Si(CH₃)₃), –0.46 (br, 12 H, Al(CH₃)₂). – $^{13}\text{C}\{^1\text{H}\}$ NMR (125 MHz, $[\text{D}_8]\text{THF}$): δ = 149.2 (s, C₁₀, C₉), 129.4–128.8 (s, C_{10a}, C_{4a}, C_{9a}, C_{8a}), 127.9 (s, C₂, C₃, C₆, C₇), 125.8 (s, C₁, C₅), 125.2 (s, C₄, C₈), 2.5 (s, Si(CH₃)₃), –4.9 (s, 4 C, Al(CH₃)₂). – EI-MS: m/z (%) = 687 (100) $[\text{M}-\text{Me}]^+$, 573 (64) $[\text{M}-\text{SiMe}_3-\text{AlMe}_2+\text{H}]^+$, 481 (52) $[\text{S}-\text{anthracene}-\text{S}]^{2+}$, 413 (53) $[\text{M}-4\text{SiMe}_3+3\text{H}]^+$, 73 (40) $[\text{SiMe}_3]^+$.

X-Ray structure determination

The data for **1–6** were collected from shock-cooled crystals at 100 K. The data for all compounds were collected on Bruker SMART-APEX II diffractometers with D8 goniometers. For the data collection of **3** a Bruker TXS-Mo rotating anode was used as X-ray source, for the others an Incoatec microfocus source was employed [39]. All diffractometers were equipped with a low-temperature device [40,41] and used monochromated $\text{MoK}\alpha$ radiation, $\lambda = 0.71073 \text{ \AA}$. Both sources used mirror optics as radiation monochromator. The data sets were integrated with SAINT [42], and an empirical absorption correction (SADABS [43]) was applied. All structures were solved by Direct Methods (SHELXS-97 [44]) and refined by full-matrix least-squares methods against F^2 (SHELXL-97 [45]). All non-hydrogen atoms were refined with anisotropic displacement parameters. The hydrogen atoms were refined isotropically on calculated positions using a riding model with their U_{iso} values constrained to 1.5 times the U_{eq} of their pivot atoms for terminal sp^3 carbon atoms and 1.2 times for all other carbon atoms. Disordered moieties were refined using bond length restraints and isotropic displacement parameter restraints.

Table 3. Crystal structure data for **1–6**.

| | 1 | 2 | 3 | 4 | 5 | 6 |
|--|--|---|--|---|---|--|
| Formula | C ₃₀ H ₄₂ BrLi- N ₂ O ₂ S | C ₅₂ H ₇₂ Br ₄ Li ₄ - N ₄ O ₂ S ₂ | C ₂₄ H ₃₂ AlBr- N ₂ S | C ₅₄ H ₉₂ Li ₂ - N ₄ O ₆ S ₂ | C ₄₂ H ₇₆ Li ₂ - N ₄ O ₄ S ₂ Si ₄ | C ₃₀ H ₅₆ Al ₂ - N ₄ S ₂ Si ₄ |
| CCDC no. | 764278 | 764279 | 764280 | 764281 | 764282 | 764283 |
| <i>M</i> _r | 581.57 | 1196.66 | 487.47 | 971.32 | 891.43 | 703.23 |
| Crystal size, mm ³ | 0.2×0.05×0.05 | 0.2×0.15×0.1 | 0.35×0.2×0.1 | 0.2×0.15×0.15 | 0.15×0.1×0.05 | 0.2×0.15×0.15 |
| Crystal system | orthorhombic | monoclinic | orthorhombic | monoclinic | monoclinic | monoclinic |
| Space group | <i>Pna</i> 2 ₁ | <i>P</i> 2 ₁ / <i>n</i> | <i>Pbca</i> | <i>P</i> 2 ₁ / <i>n</i> | <i>P</i> 2 ₁ / <i>n</i> | <i>P</i> 2 ₁ / <i>n</i> |
| <i>a</i> , Å | 17.088(3) | 12.869(3) | 11.6435(11) | 10.5726(17) | 13.5712(14) | 9.4066(9) |
| <i>b</i> , Å | 11.1177(17) | 15.765(3) | 14.2039(13) | 17.182(3) | 10.7302(11) | 20.374(2) |
| <i>c</i> , Å | 15.878(2) | 14.182(3) | 29.779(3) | 16.000(3) | 18.6907(18) | 11.5702(12) |
| β, deg | 90 | 94.951(3) | 90 | 95.455(2) | 107.339(2) | 95.455(2) |
| <i>V</i> , Å ³ | 3016.5(8) | 2866.5(11) | 4925.0(8) | 2893.5(8) | 2598.1(5) | 2053.8(4) |
| <i>Z</i> | 4 | 2 | 8 | 2 | 2 | 2 |
| <i>D</i> _{calcd} , g cm ⁻³ | 1.28 | 1.39 | 1.32 | 1.12 | 1.14 | 1.14 |
| μ(MoKα), cm ⁻¹ | 1.5 | 2.9 | 1.8 | 0.1 | 0.2 | 0.3 |
| <i>F</i> (000), e | 1224 | 1224 | 2032 | 1060 | 964 | 756 |
| <i>hkl</i> range | 0 ≤ <i>h</i> ≤ +20 0 ≤ <i>k</i> ≤ +13 −19 ≤ <i>l</i> ≤ +19 | −16 ≤ <i>h</i> ≤ +16 0 ≤ <i>k</i> ≤ +19 0 ≤ <i>l</i> ≤ +17 | 0 ≤ <i>h</i> ≤ +14 0 ≤ <i>k</i> ≤ +17 0 ≤ <i>l</i> ≤ +37 | −13 ≤ <i>h</i> ≤ +12 0 ≤ <i>k</i> ≤ +21 −19 ≤ <i>l</i> ≤ +19 | −16 ≤ <i>h</i> ≤ +15 0 ≤ <i>k</i> ≤ +12 0 ≤ <i>l</i> ≤ +22 | −11 ≤ <i>h</i> ≤ +11 0 ≤ <i>k</i> ≤ +25 0 ≤ <i>l</i> ≤ +14 |
| ((sin θ)/λ) _{max} , Å ⁻¹ | 25.41 | 26.44 | 26.44 | 26.02 | 25.39 | 26.75 |
| Refl. measured | 35006 | 43137 | 58664 | 31291 | 30165 | 48448 |
| Refl. unique | 5563 | 5893 | 5056 | 5681 | 4750 | 4353 |
| <i>R</i> _{int} | 0.0990 | 0.0550 | 0.0428 | 0.0392 | 0.0521 | 0.0344 |
| Param. refined | 340 | 335 | 270 | 341 | 268 | 198 |
| <i>R</i> (<i>F</i>) / <i>wR</i> (<i>F</i> ²) ^a (all refl.) | 0.0666 / 0.1461 | 0.0480 / 0.1124 | 0.0533 / 0.1235 | 0.0669 / 0.1500 | 0.0535 / 0.1088 | 0.0343 / 0.0746 |
| χ(Flack) [46, 47] | 0.026(12) | – | – | – | – | – |
| GoF (<i>F</i> ²) ^b | 1.049 | 1.079 | 1.019 | 1.082 | 1.040 | 1.099 |
| Δρ _{fin} (max / min), e Å ⁻³ | 0.51 / −0.94 | 1.08 / −1.10 | 0.94 / −1.14 | 0.50 / −0.52 | 0.41 / −0.32 | 0.32 / −0.22 |

^a $R1 = \sum ||F_o| - |F_c|| / \sum |F_o|$, $wR2 = [\sum w(F_o^2 - F_c^2)^2 / \sum w(F_o^2)^2]^{1/2}$, $w = [\sigma^2(F_o^2) + (AP)^2 + BP]^{-1}$, where $P = (\text{Max}(F_o^2, 0) + 2F_c^2) / 3$ and A and B are constants adjusted by the program; ^b $\text{GoF} = S = [\sum w(F_o^2 - F_c^2)^2 / (n_{\text{obs}} - n_{\text{param}})]^{1/2}$, where n_{obs} is the number of data and n_{param} the number of refined parameters.

Crystal data and parameters pertinent to data collection and structure refinement are summarized in Table 3.

CCDC 764278–764283 contain the supplementary crystallographic data for this paper. These data can be obtained free of charge from The Cambridge Crystallographic Data Centre via www.ccdc.cam.ac.uk/data_request/cif.

Acknowledgement

The authors like to thank the Georg-August Universität Göttingen, the Land Niedersachsen and the Volkswagenstiftung for supplying superb X-ray facilities.

- | | |
|--|--|
| <p>[1] F.M. Piller, A. Metzger, M. A. Schade, B. A. Haag, A. Gavryushin, P. Knochel, <i>Chem. Eur. J.</i> 2009, <i>15</i>, 7192–7202.</p> <p>[2] S.H. Wunderlich, M. Kienle, P. Knochel, <i>Angew. Chem.</i> 2009, <i>121</i>, 7392–7396; <i>Angew. Chem. Int. Ed.</i> 2009, <i>48</i>, 7256–7260.</p> <p>[3] P. Knochel, W. Dohle, N. Gommermann, F.F. Kneisel, F. Kopp, T. Korn, I. Sapountzis, V.A. Vu, <i>Angew. Chem.</i> 2003, <i>115</i>, 4438–4456; <i>Angew. Chem. Int. Ed.</i> 2003, <i>42</i>, 4302–4320.</p> <p>[4] D.R. Armstrong, E. Herd, D.V. Graham, E. Hevia, A.R. Kennedy, W. Clegg, L. Russo, <i>Dalton Trans.</i> 2008, 1323–1330.</p> <p>[5] W. Clegg, J. Garcia-Alvarez, P. Garcia-Alvarez, D.V. Graham, R.W. Harrington, E. Hevia, A.R. Kennedy,</p> | <p>R.E. Mulvey, L. Russo, <i>Organometallics</i> 2008, <i>27</i>, 2654–2663.</p> <p>[6] R.E. Mulvey, F. Mongin, M. Uchiyama, Y. Kondo, <i>Angew. Chem.</i> 2007, <i>119</i>, 3876–3899; <i>Angew. Chem. Int. Ed.</i> 2007, <i>46</i>, 3802–3825.</p> <p>[7] P.C. Andrikopoulos, D.R. Armstrong, D.V. Graham, E. Hevia, A.R. Kennedy, R.E. Mulvey, C.T. O'Hara, C. Talmard, <i>Angew. Chem.</i> 2005, <i>117</i>, 3525–3528; <i>Angew. Chem. Int. Ed.</i> 2005, <i>44</i>, 3459–3462.</p> <p>[8] S. Podder, S. Roy, <i>Tetrahedron</i> 2007, <i>63</i>, 9146–9152.</p> <p>[9] D. Prim, B. Andrioletti, F.R.-M. Rose-Munch, E. Rose, F. Couty, <i>Tetrahedron</i> 2004, <i>60</i>, 3325–3347.</p> <p>[10] N. Yamagiwa, S. Matsunaga, M. Shibasaki, <i>J. Am. Chem. Soc.</i> 2003, <i>125</i>, 16178–16179.</p> <p>[11] W.K. Chan, <i>Coord. Chem. Rev.</i> 2007, <i>251</i>, 2104–2118.</p> |
|--|--|

- [12] M. Al-Anber, T. Stein, S. Vatsadze, H. Lang, *Inorg. Chim. Acta* **2005**, 358, 50–56.
- [13] R. Fleischer, S. Freitag, D. Stalke, *J. Chem. Soc., Dalton Trans.* **1998**, 193–197.
- [14] R. Fleischer, S. Freitag, F. Pauer, D. Stalke, *Angew. Chem.* **1996**, 108, 208–211; *Angew. Chem., Int. Ed. Engl.* **1996**, 35, 204–207.
- [15] J. A. Hunter, B. King, W. E. Lindsell, M. A. Neish, *J. Chem. Soc., Dalton Trans.* **1980**, 880–887.
- [16] M. Shibasaki, H. Sasai, T. Arai, T. Iida, *Pure Appl. Chem.* **1998**, 70, 1027–1034.
- [17] M. Shibasaki, H. Sasai, T. Arai, *Angew. Chem.* **1997**, 109, 1290–1311; *Angew. Chem., Int. Ed. Engl.* **1997**, 36, 1235–1256.
- [18] S.-J. Liu, Q. Zhao, B.-X. Mi, W. Huang, *Adv. Polym. Sci.* **2008**, 212, 125–144.
- [19] I. Manners, *Angew. Chem.* **1996**, 108, 1712–1731; *Angew. Chem., Int. Ed. Engl.* **1996**, 35, 1602–1621.
- [20] T. Schulz, D. Dauer, D. Stalke, *Z. Naturforsch.* **2010**, 65b, 711–718.
- [21] C. Selinka, D. Stalke, *Eur. J. Inorg. Chem.* **2003**, 3376–3382.
- [22] B. Walfort, R. Bertermann, D. Stalke, *Chem. Eur. J.* **2001**, 7, 1424–1430.
- [23] G. Schwab, D. Stern, D. Leusser, D. Stalke, *Z. Naturforsch.* **2007**, 62b, 711–716.
- [24] G. Schwab, PhD thesis, University of Göttingen, Göttingen, **2008**.
- [25] R. Fleischer, D. Stalke, *J. Organomet. Chem.* **1998**, 550, 173–182.
- [26] R. Fleischer, D. Stalke, *Coord. Chem. Rev.* **1998**, 176, 431–450.
- [27] C. Selinka, S. Deuerlein, T. Häuser, D. Stalke, *Inorg. Chim. Acta* **2004**, 357, 1873–1880.
- [28] B. Walfort, A. P. Leedham, C. R. Russell, D. Stalke, *Inorg. Chem.* **2001**, 40, 5668–5674.
- [29] G. R. Desiraju, T. Steiner, *The Weak Hydrogen Bond*, IUCr Monographs on Crystallography, Vol. 9, Oxford University Press, Oxford, **1999**.
- [30] B. Walfort, T. Auth, B. Degel, H. Helten, D. Stalke, *Organometallics* **2002**, 21, 2208–2214.
- [31] S. Freitag, W. Kolodziejcki, F. Pauer, D. Stalke, *J. Chem. Soc., Dalton Trans.* **1993**, 3479–3488.
- [32] F. T. Edelmann, F. Knösel, F. Pauer, D. Stalke, W. Bauer, *J. Organomet. Chem.* **1992**, 438, 1–10.
- [33] F. Pauer, D. Stalke, *J. Organomet. Chem.* **1991**, 418, 127–128.
- [34] H. Ott, C. Däschlein, D. Leusser, D. Schildbach, T. Seibel, D. Stalke, C. Strohmann, *J. Am. Chem. Soc.* **2008**, 130, 11901–11911.
- [35] A. F. Holleman, N. Wiberg, *Lehrbuch der Anorganischen Chemie*, 102. Aufl., de Gruyter, Berlin, **2007**.
- [36] G. Schwab, D. Stern, D. Stalke, *J. Org. Chem.* **2008**, 73, 5242–5247.
- [37] O. J. Scherer, G. Wolmershäuser, *Z. Anorg. Allg. Chem.* **1977**, 432, 173–176.
- [38] O. J. Scherer, R. Wies, *Z. Naturforsch.* **1970**, 25b, 1486–1487.
- [39] T. Schulz, K. Meindl, D. Leusser, D. Stern, J. Graf, C. Michaelson, M. Ruf, G. M. Sheldrick, D. Stalke, *J. Appl. Crystallogr.* **2009**, 42, 885–891.
- [40] T. Kottke, R. J. Lagow, D. Stalke, *J. Appl. Crystallogr.* **1996**, 29, 465–468.
- [41] T. Kottke, D. Stalke, *J. Appl. Crystallogr.* **1993**, 26, 615–619.
- [42] SAINT v7.46A, Bruker Analytical X-ray Instruments Inc., Madison, Wisconsin (USA) **2007**.
- [43] G. M. Sheldrick, SADABS (version 2008/2), Program for Empirical Absorption Correction of Area Detector Data, University of Göttingen, Göttingen (Germany) **2008**.
- [44] G. M. Sheldrick, textscShelxs-97, Program for the Solution of Crystal Structures, University of Göttingen, Göttingen (Germany) **1997**. See also: G. M. Sheldrick, *Acta Crystallogr.* **1990**, A46, 467–473.
- [45] G. M. Sheldrick, SHELXL-97, Program for the Refinement of Crystal Structures, University of Göttingen, Göttingen (Germany) **1997**. See also: G. M. Sheldrick, *Acta Crystallogr.* **2008**, A64, 112–122.
- [46] G. Bernardinelli, H. D. Flack, *Acta Crystallogr.* **1985**, A41, 500–511.
- [47] H. D. Flack, *Acta Crystallogr.* **1983**, A39, 876–881.